

University of Dundee

## Quantitative assessment of the conjunctival microcirculation using a smartphone and slit-lamp biomicroscope

Brennan, Paul F.; Mcneil, Andrew J.; Jing, Min; Awuah, Agnes; Finlay, Dewar D.; Blighe, Kevin

*Published in:*  
Microvascular Research

*DOI:*  
[10.1016/j.mvr.2019.103907](https://doi.org/10.1016/j.mvr.2019.103907)

*Publication date:*  
2019

*Licence:*  
CC BY-NC-ND

*Document Version*  
Peer reviewed version

[Link to publication in Discovery Research Portal](#)

### *Citation for published version (APA):*

Brennan, P. F., Mcneil, A. J., Jing, M., Awuah, A., Finlay, D. D., Blighe, K., McLaughlin, J. A. D., Wang, R., Moore, J. E., Nesbit, M. A., Trucco, E., Spence, M. S., & Moore, C. B. T. (2019). Quantitative assessment of the conjunctival microcirculation using a smartphone and slit-lamp biomicroscope. *Microvascular Research*, 126, 1-5. [103907]. <https://doi.org/10.1016/j.mvr.2019.103907>

### **General rights**

Copyright and moral rights for the publications made accessible in Discovery Research Portal are retained by the authors and/or other copyright owners and it is a condition of accessing publications that users recognise and abide by the legal requirements associated with these rights.

- Users may download and print one copy of any publication from Discovery Research Portal for the purpose of private study or research.
- You may not further distribute the material or use it for any profit-making activity or commercial gain.
- You may freely distribute the URL identifying the publication in the public portal.

### **Take down policy**

If you believe that this document breaches copyright please contact us providing details, and we will remove access to the work immediately and investigate your claim.

**Manuscript title**    Quantitative assessment of the conjunctival microcirculation  
using a smartphone and slit-lamp biomicroscope

### **Highlights**

- The conjunctiva has a readily-accessible microcirculation for haemodynamic analysis
- Smartphone-assisted haemodynamic assessment of the conjunctiva is feasible
- Increasing conjunctival vessel diameter results in increased blood volume flow
- Wall shear rate decreases as conjunctival vessel diameter increases

**Title Page**

**Manuscript title** Quantitative assessment of the conjunctival microcirculation using a smartphone and slit-lamp biomicroscope

**Author list (in order)**

1. Dr Paul F. Brennan<sup>a,b</sup> [paul.brennan@belfasttrust.hscni.net](mailto:paul.brennan@belfasttrust.hscni.net)
2. Dr Andrew J. McNeil<sup>c</sup> [a.y.mcneil@dundee.ac.uk](mailto:a.y.mcneil@dundee.ac.uk)
3. Dr Min Jing<sup>d</sup> [m.jing@ulster.ac.uk](mailto:m.jing@ulster.ac.uk)
4. Miss Agnes Awuah<sup>a</sup> [awuah-a@ulster.ac.uk](mailto:awuah-a@ulster.ac.uk)
5. Professor Dewar D. Finlay<sup>d</sup> [d.finlay@ulster.ac.uk](mailto:d.finlay@ulster.ac.uk)
6. Professor Kevin Blighe<sup>a</sup> [k.blighe@ulster.ac.uk](mailto:k.blighe@ulster.ac.uk)
7. Professor James A.D McLaughlin<sup>d</sup> [jad.mclaughlin@ulster.ac.uk](mailto:jad.mclaughlin@ulster.ac.uk)
8. Professor Ruixuan Wang<sup>c</sup> [ruixuan.wang@hotmail.com](mailto:ruixuan.wang@hotmail.com)
9. Professor Jonathan Moore<sup>a</sup> [johnny@cathedraleye.com](mailto:johnny@cathedraleye.com)
10. Dr M. Andrew Nesbit<sup>a</sup> [a.nesbit@ulster.ac.uk](mailto:a.nesbit@ulster.ac.uk)
11. Professor Emanuele Trucco<sup>c</sup> [e.trucco@dundee.ac.uk](mailto:e.trucco@dundee.ac.uk)
12. Dr Mark S. Spence<sup>b</sup> [marks.spence@belfasttrust.hscni.net](mailto:marks.spence@belfasttrust.hscni.net)
13. Professor Tara C.B. Moore<sup>a</sup> [tara.mcmullen@ulster.ac.uk](mailto:tara.mcmullen@ulster.ac.uk)

**Corresponding author** Professor Tara C.B. Moore<sup>a</sup>

[tara.mcmullen@ulster.ac.uk](mailto:tara.mcmullen@ulster.ac.uk)

**Institutions** <sup>a</sup> Biomedical Sciences Research Institute, Ulster University, Coleraine, United Kingdom, BT521SA

<sup>b</sup> Department of Cardiology, Royal Victoria Hospital, Belfast Health and Social Care Trust, Belfast, United Kingdom, BT126BA

25 <sup>c</sup> *VAMPIRE project, Computing (SSEN), University of Dundee, Dundee, United*  
26 *Kingdom, DD1 4HN*

27 <sup>d</sup> *Nanotechnology and Integrated Bioengineering Centre (NIBEC), Ulster University,*  
28 *Jordanstown, United Kingdom, BT37 0QB*

29

30

31 **Wordcount** 3449 words (excluding abstract, acknowledgements and  
32 references)

33

34

35 **Funding** This project was funded by Northern Ireland Chest Heart and Stroke  
36 (NICHHS), the Ulster University and the Heart Trust fund, Royal Victoria Hospital,  
37 Belfast, United Kingdom.

38

39 **Keywords** Conjunctival circulation; microcirculation; smartphone;  
40 haemodynamic assessment; endothelial dysfunction

## Abstract

**Purpose** The conjunctival microcirculation is a readily-accessible vascular bed for quantitative haemodynamic assessment and has been studied previously using a digital charge-coupled device (CCD). Smartphone video imaging of the conjunctiva, and haemodynamic parameter quantification, represents a novel approach. We report the feasibility of smartphone video acquisition and subsequent haemodynamic measure quantification via semi-automated means.

**Methods** Using an Apple iPhone 6s and a Topcon SL-D4 slit-lamp biomicroscope, we obtained videos of the conjunctival microcirculation in 4 fields of view per patient, for 17 low cardiovascular risk patients. After image registration and processing, we quantified the diameter, mean axial velocity, mean blood volume flow, and wall shear rate for each vessel studied. Vessels were grouped into quartiles based on their diameter i.e. group 1 ( $<11\mu\text{m}$ ), 2 ( $11\sim16\mu\text{m}$ ), 3 ( $16\sim22\mu\text{m}$ ) and 4 ( $>22\mu\text{m}$ ).

**Results** From the 17 healthy controls (mean QRISK3 6.6%), we obtained quantifiable haemodynamics from 623 vessel segments. The mean diameter of microvessels, across all sites, was  $18.23\mu\text{m}$  (range  $6.6\text{-}39.2\mu\text{m}$ ). Mean axial velocity was  $0.49\text{mm/s}$  (range  $0.12\text{-}0.79\text{mm/s}$ ) and there was a modestly positive correlation ( $r\ 0.404$ ) seen with increasing diameter, best appreciated when comparing group 4 to the remaining groups ( $p<0.0001$ ). Blood volume flow (mean  $109.718\text{pl/s}$ , range  $11.28\text{-}502.19\text{pl/s}$ ) was strongly correlated with increasing diameter ( $r\ 0.967$ ,  $p<0.0001$ ) and wall shear rate (mean  $182.81\text{s}^{-1}$ , range  $55.11\text{-}546.69\text{s}^{-1}$ ) negatively correlated with increasing diameter ( $r\ -0.823$ ,  $p<0.0001$ ).

**Conclusions** We, for the first time, report the successful assessment and quantification of the conjunctival microcirculatory haemodynamics using a smartphone-based system.

## **Manuscript**

### **I. Introduction**

Cardiovascular disease (CVD) is a leading cause, globally, of mortality and morbidity while also being associated with a significant economic burden on health services<sup>1</sup>. CVD is caused by physiological changes and endothelial dysfunction, resulting in atherosclerosis, and it is accepted that these changes manifest earliest in the microcirculatory networks within the body<sup>2</sup>. Microcirculatory disease typically commences with endothelial dysfunction which may be clinically silent and, thus, precede the onset of symptoms<sup>3</sup> or the occurrence of a major adverse cardiovascular event (MACE) e.g. myocardial infarction (MI) or cerebrovascular accident (CVA). Microvascular dysfunction is associated with increased mortality<sup>4</sup> and thus the study of microcirculations may provide a potential tool in disease screening, staging and management. Imaging of systemic microcirculations has been applied to and, in certain disease subsets, is used in every day current practice in assessing disease progression e.g. the retinal microcirculation in the assessment of diabetes mellitus, systemic hypertension, and sickle cell disease<sup>5,6,7,8</sup>. The sublingual mucosa and the skin also represent accessible sites in which the microcirculation has been studied by videomicroscopy<sup>9</sup>. The anterior segment of the eye contains the conjunctival microvasculature, a readily-accessible heterogeneous network of arterioles and venules adjacent to the limbal microcirculation, which gains its supply from the anterior ciliary branch of the

ophthalmic artery<sup>10</sup>. The conjunctival microvasculature allows for both non-invasive assessment of erythrocyte movement, and quantification of key vascular physiological parameters e.g. vessel width, blood flow axial velocity and blood flow rate<sup>11</sup>.

The objective of this study was to evaluate the feasibility of assessing the conjunctival microcirculation using our novel combination of a smartphone and slit-lamp biomicroscope. We aimed to develop an operator-friendly, pragmatic, safe and effective means of assessing this heterogeneous circulation, in addition to the quantification of the haemodynamic physiological parameters seen within a microcirculation.

A few groups have reported semi-automated or automated image analysis algorithms to assess the conjunctival microcirculation, using a slit lamp biomicroscope and a digital charge-coupled device (CCD) camera for image acquisition<sup>12,13,14,15,16,17</sup>. Using such systems, the conjunctival microcirculation has been studied in patients with hypertension, diabetic retinopathy, and patients after ischaemic stroke<sup>18, 19, 20</sup>. In addition, one group has reported the application of such methods in patients of varying predictive cardiovascular risk, assessed by the Framingham risk score<sup>21</sup>.

Smartphone technology allows for remote monitoring and screening of many prevalent cardiovascular conditions, for example atrial fibrillation, and represents an important component of future healthcare and cardiovascular practice<sup>22</sup>. The literature is scarce regarding smartphone use to assess microcirculatory haemodynamics but the application of smartphone photography of the fundus has been reported in diabetic and hypertensive patients<sup>23, 24, 25</sup>. There are some studies describing smartphone-led image analysis of the conjunctiva in the assessment of

patients with anaemia<sup>26,27</sup> and, also, quantification of conjunctival “redness” i.e. hyperaemia<sup>28</sup>. In addition, the smartphone-based biometric has been studied on the visible vascular patterns on whites of the eye<sup>29</sup> but, at this time, there are no studies that describe the assessment or quantification of conjunctival haemodynamics using a smartphone and slit-lamp combination.

## **II. Materials and Methods**

### **A. Subjects**

This research study was approved by the Research and Development review boards of the Ulster University (UU) and the Belfast Health and Social Care Trust (BHSCT). All subjects were provided with verbal and written information, prior to study enrolment, in accordance with the Declaration of Helsinki. Exclusion criteria included inability to consent, prior myocardial infarction (MI), uncontrolled systemic hypertension, recent history of conjunctival inflammation, prior refractive surgery, used ocular medications (other than artificial tears) and current use of contact lenses.

We recruited 17 healthy volunteers to this feasibility study. The mean age for the population studied was  $52.5 \pm 10.3$  years, IQR 15 years. Sex distribution was roughly equal with 9 (53%) males and 8 females (47%). No patients had a history of prior MI, cerebrovascular accident (CVA), or diabetes mellitus. The QRISK 3 (<https://qrisk.org/three/>) score algorithm was used to estimate each volunteer’s 10-year risk of future heart attack or stroke. The QRISK 3 algorithm is based on the presence/lack of specific risk factors for CVD e.g. smoking, diabetes mellitus, hypertension, family history angina, chronic kidney disease, age, sex, body mass index, history of atrial fibrillation, use of regular steroid tablets, presence of chronic



inflammatory disease, and cholesterol profile. It has been well-validated in our population<sup>30</sup>. The mean QRISK 3 score was 6.6 ±9%, IQR 6.9%, which correlates with a “low-risk” population (<10%). Table 1 is a summary of the baseline demographics and clinical observations for the study group.

	Number n=17
<i>Male sex, n (%)</i>	9 (53.0)
<i>Age, years ±SD</i>	52.5 ±10.3
<i>QRISK 3 score, % ±SD</i>	6.6 ±9
<i>Systolic blood pressure, mmHg ±SD</i>	125 ±22
<i>Diastolic blood pressure, mmHg ±SD</i>	77 ±12
<i>Heart rate, bpm ±SD</i>	70 ±9
<i>Prior MI/CVA/Diabetes mellitus</i>	0

Table 1. Baseline characteristics of the study group (n=17) with continuous variables expressed using their mean and standard deviation. Categorical variables have been expressed as a number and percentage of the total within that variable.

### **B. Image Acquisition**

Image acquisition was achieved via two main hardware components. Firstly, primary illumination and magnification of the ocular vascular structure was achieved using a conventional slit lamp biomicroscope, Topcon SL-D4 (Topcon Medical Systems Inc., USA), capable of providing a maximum magnification of 40x. Secondly, images provided by the slit lamp biomicroscope were further magnified and stored using a smartphone camera. The smartphone used in the system is an Apple iPhone 6s (Apple, Inc., USA). A number of video record settings were tested and the optimal configuration set at a resolution of 1920 x 1080 pixels, captured at 60 frames per second. The iPhone video recorder is capable of providing a further magnification of

3x. Coupling of the smartphone to the eyepiece of the slit lamp biomicroscope was achieved using a bespoke adapter developed by Zarf Enterprises (Zarf Enterprises., USA). Smartphone cameras typically give very little control over camera properties (focus, ISO, shutter speed, aperture) due to an emphasis on ease-of-use for everyday consumers, while also generating compressed video files (h.264 compression in the case of the iPhone 6s). To help overcome these issues we captured our data using a third-party application "ProMovie Recorder" ([www.promovieapp.com](http://www.promovieapp.com)). We used constant settings for all images (iso/shutter speed/ focus/ exposure) and used the maximum compression bit-rate available to reduce compression artefacts. The video zoom setting was locked at 2x, providing a 1:1-pixel mapping of the camera sensor at 1080p resolution and thus avoiding interpolation artefacts. To obtain an accurate pixel to mm conversion factor we calibrated the system using a digital caliper and 1mm microscope calibration reticle, deriving a conversion factor of  $552 \pm 22.6$  pixels/mm. We obtained one video (5-15s) from 4 distinct field of views i.e. medial and temporal conjunctiva in both eyes. Fig.1. To reduce eye motion and blinking we used an external fixation target as a focal point for each patient. We acquired only 4 videos (5-15s) per patient to minimise the risk of potential adverse effects, e.g. slit-lamp light exposure. There were no reported adverse effects at the time of, or after, image acquisition. Patients were imaged in the same clinical room under constant temperature and lighting settings.

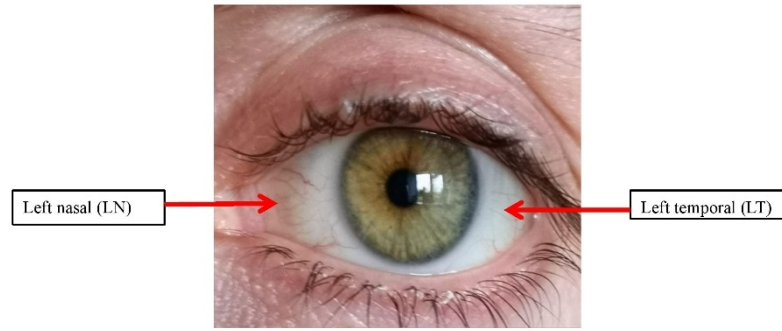


Fig. 1. Two fields of view (FOV) for the left eye of a healthy subject, with the medial and lateral FOV being labelled (red arrows) the left nasal (LN) and left temporal (LT) respectively.

### **C. Image Processing**

#### **1. Pre-Processing and Vessel Segmentation**

An initial pre-processing procedure was carried out for each video file. Firstly, the longest stable sequence of frames was manually selected on the basis of the vasculature being in focus, there being no blinking or large sudden movements of the eye, and the FOV not drifting by more than ~25% of the width of the frame. Next the green channel, which gave the highest vessel contrast, was extracted and information from the red channel used to correct for uneven illumination through subtraction. The sharpest frame in the sequence was then selected as a reference frame and all other frames registered to it through an affine registration procedure<sup>31</sup>, with a single composite image generated by averaging all registered frames. After applying a “vessel enhancement filter”<sup>32</sup> (Fig.2 (a)), a binary map of the conjunctival

vasculature and corresponding centrelines were obtained via standard skeletisation techniques. Finally, the connected vessel network was broken into individual vessel segments (Fig.2 (b)) by setting the branch points' neighbouring pixels to zero, and centreline segments, containing more than 30 pixels, selected for further assessment.

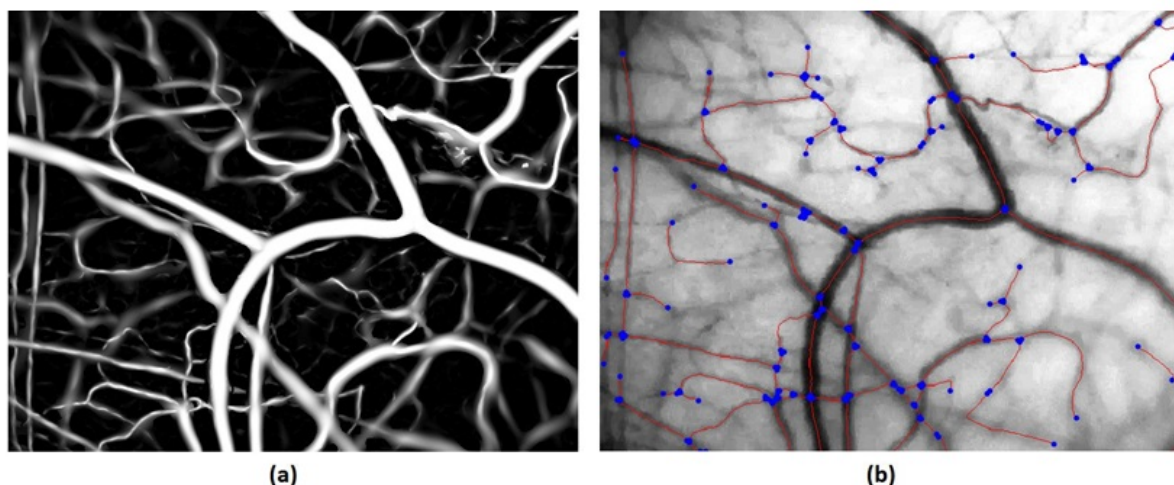


Fig. 2. Microvascular network after image processing: (a) the vessel network after filtering; (b) the vessel centreline (in red) and intersection points (in blue) overlaid on the mean of vessel images.

## 2. Vessel Diameter (D)

The Euclidean Distance Transform (EDT) was proposed for vessel diameter estimation, which is easier to implement in comparison to the commonly used method via full width at half maximum (FWHM). The value at each pixel of EDT was calculated based on the Euclidean distance between the pixel and its nearest nonzero pixel in the binary vessel image. The centreline of the vessel was used to obtain the central EDT values and thus the radius along the vessel axis. The average of diameters along the vessel length provided the final vessel width estimation. An example based on simulation is illustrated in Fig.3.

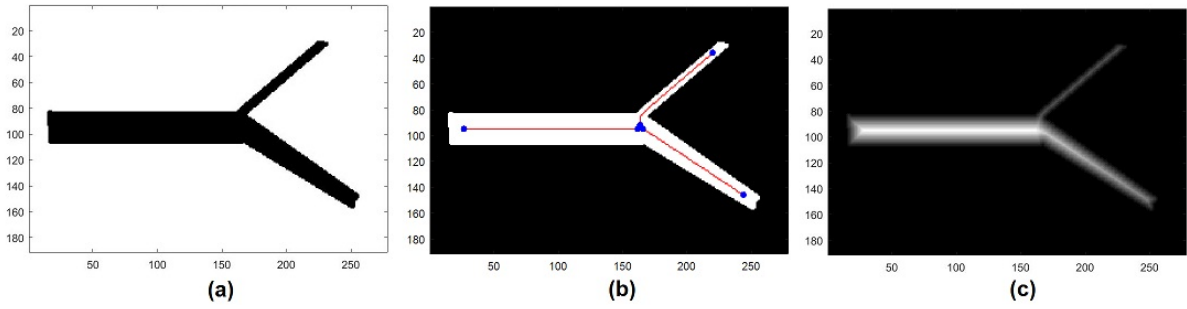


Fig. 3. Simulation for vessel diameter estimation: (a) three vessels are generated with mean diameter 25.3 pixels, 16.5 pixels, and 8.3 pixels, respectively; (b) the vessel centreline, end points and branch points overlaid on the binary vessel image; (c) EDT of the binary vessel image. The mean of estimated diameters via EDT are 25.9 pixels, 16.6 pixels, and 8.6 pixels, respectively.

Given the complex and heterogeneous distribution of conjunctival microvessels, we applied a grouping classification to our results, described in previous work, based on vessel D i.e. group 1 ( $<11\mu\text{m}$ ), group 2 ( $11\text{--}16\mu\text{m}$ ), group 3 ( $16\text{--}22\mu\text{m}$ ) and group 4 ( $>22\mu\text{m}$ )<sup>11</sup>.

### 3. Axial velocity ( $V_a$ )

The blood flow  $V_a$  in a single vessel segment was estimated based on the spatial-temporal image (STI), with the change in intensity in STI reflecting erythrocyte movement through the vessel. Since STI signal is the one dimension of space plus time, i.e., a 1D+T signal, a novel approach based on spatial temporal 1D+T continuous wavelet transform (1DTCWT) is proposed for  $V_a$  estimation. The CWT method has been used previously as a spatiotemporal filter for motion capture of 1D+T signals for moving target tracking and parameter calculation<sup>33</sup>, but not yet exploited in microvascular blood flow velocity estimation. Firstly, 2D fast Fourier transform (FFT) is performed for STI. The velocity vector space is defined and

1DTCWT is then run at each time interval. The energy is subsequently calculated based on the 1DTCWT output. The velocity is obtained by searching the maximum energy point as shown in Fig.4. The average of the absolute velocity across all frames was used as the final estimation of  $V_a$ . The method was programmed in MATLAB2017 together with an open source implementation of CWT <sup>34</sup>.

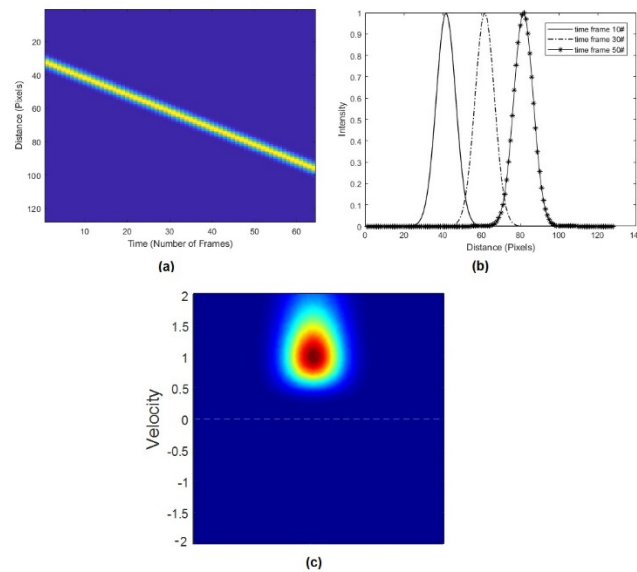


Fig.4. Simulation for velocity estimation based on 1DTCWT. (a) synthetic STI generated by shifting Gaussian signal with speed of 1 pixel/frame; (2) plot of signals at the 10th, 30th and 50th frames, which shows the Gaussian signal shifting in distance; (c) a colour spectrum map via 1DTCWT shows the velocity is corresponding to the maximum of the energy (at 1 pixel/frame).

#### 4. Blood flow (Q) and wall shear rate (WSR)

Using the measurements for  $D$  and  $V_a$ , we calculated  $Q$  and WSR using previously described methods <sup>11,12</sup>.  $Q$  provides key information regarding the architecture and function of the vascular system, whereas WSR is the blood velocity at a specific wall

position, within a vessel, and represents a surrogate for the pressure exerted by blood within its' respective transport vessel<sup>35, 36, 37</sup>.

## 5. Statistical analysis

For statistical analysis SPSS for Apple iOS version 25 (property of IBM) and R version 3.5.3 ([www.r-project.org](http://www.r-project.org)) were used. Continuous variables were described using the mean, standard deviation of the mean and interquartile range (IQR) for the variable. Categorical variables were described as a number and percentage of the total category number to which the variable belonged. Sample origin, distribution and variance were assessed by non-parametric ANOVA (Kruskal-Wallis test). Correlation analysis (Spearman rank), with a Loess regression fit, was applied to assess relationships between D and independent variables, principally Va, Q and WSR. Non-parametric ANOVA (Kruskal-Wallis) with or without Dunn's post-hoc tests was used to compare D, Va, W, and WSR by vessel width group, with the tests being conducted separately across site, i.e., left/right nasal and temporal, or for all sites merged.

## III. Results

For the 17 healthy patients studied, using our semi-automated approach, we were able to obtain repeated measurements in 623 vessel segments (mean 37 segments per patient), hereafter referred to as "microvessels", which exhibited observable flow. The mean diameter (D) of microvessels, across all sites, was 18.2 $\mu$ m (range 6.6-39.2 $\mu$ m). Group 4 (>22 $\mu$ m) microvessels were measured most frequently, with group 1 (<11 $\mu$ m) being the least commonly encountered i.e. 295 vs 64 microvessels respectively. Mean Va was 0.49mm/s (range 0.12-0.79mm/s), Q 109.72pl/s (range

11.28-502.19pl/s) and WSR ranged between 55.11-546.69s<sup>-1</sup>, with a mean WSR of 182.81s<sup>-1</sup>. The mean and SD of all microvessel conjunctival haemodynamic parameters are illustrated in Table 2. Statistical comparisons for Va, Q and WSR were made within the vessel groups. There was a statistically significant increase in Q for increasing diameter size (p<0.0001), with a statistically significant inverse correlation between WSR and increasing diameter size (p<0.0001). Va tended to increase with increasing microvessel diameter and was significantly elevated in group 4 (>22μm) vessels, compared to the remaining three groups (p<0.0001).

Group D μm	No. vessels N=623	D (μm)	Va (mm/s)	Q (pl/s)	WSR (s <sup>-1</sup> )
<11 Group 1	64	9.1 ±2.8	0.45 ±0.05	23.65 ±2.96	332.75 ±60.75
11~16 Group 2	113	13.44±3.7	0.44 ±0.06	46.81 ±8.02	200.19 ±32.89
16~22 Group 3	151	19.2 ±3.5	0.47 ±0.06	97.13 ±17.21	136.67 ±20.35
>22 Group 4	295	26.9 ±2.7	0.56 ±0.09	224.45 ±66.35	115.27 ±17.7
			p<0.0001	p<0.0001	p<0.0001
	<b>Mean</b>	18.2	0.485	109.718	182.81
	<b>Range</b>	6.6-39.2	0.12-0.79	11.28-502.19	55.11-546.69
	<b>Interquartile range (IQR)</b>	12.74-24	0.42-0.55	39.86-161	116.33- 221.72



Table 2. Summary of haemodynamic measures D, Va, Q and WSR based on the vessel diameter groups (1-4).

Across site (field of view) comparisons were made with the haemodynamic measures. Q and WSR did not statistically differ between the 4 image fields. There was a statistically higher Va noted in the right nasal (RN) hemisphere compared to the left nasal (LN, ( $p = 0.0003$ )), for which the clinical significance is unknown and may require further exploration. The relationship between the haemodynamic measures and similarities for each field of view is shown in Fig.5. Note the elevated Va in the RN FOV, compared to the other FOVs, as before.

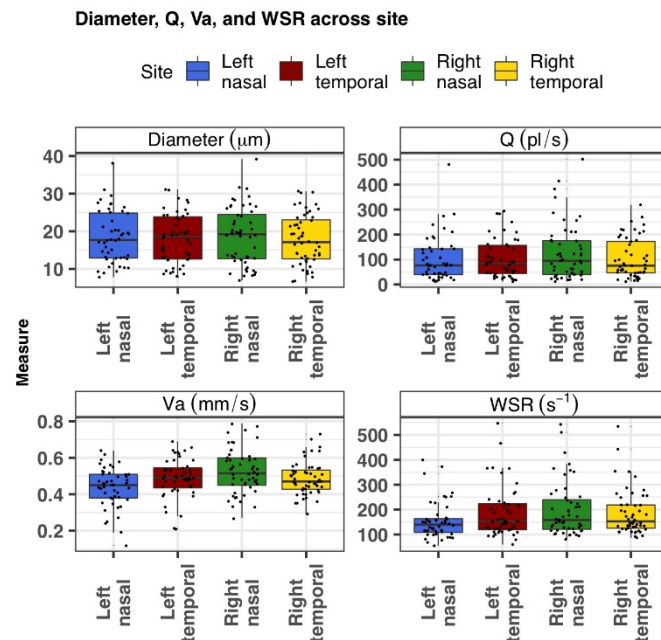
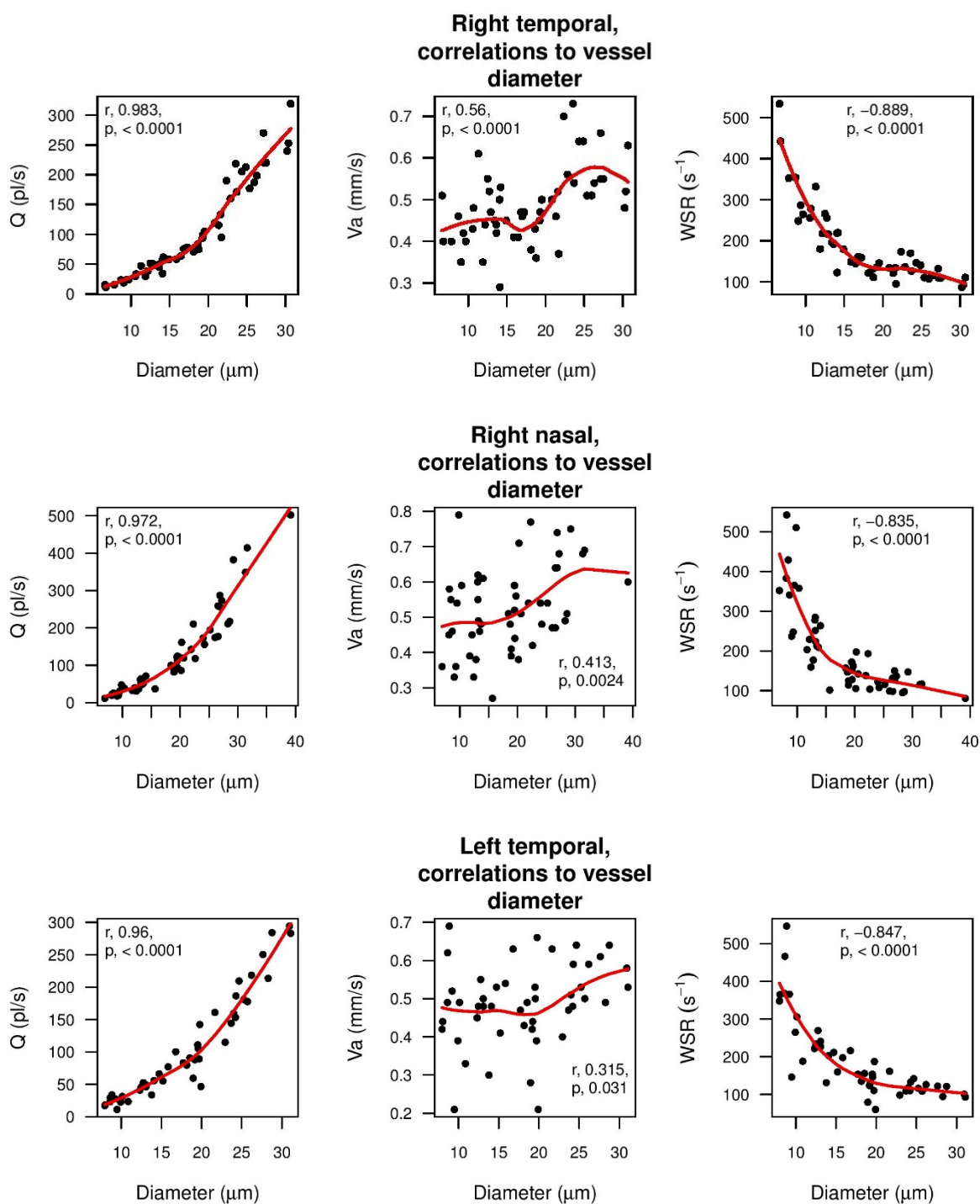


Fig.5. Summary of diameter D ( $\mu\text{m}$ ), Va ( $\text{mm/s}$ ), Q ( $\text{pl/s}$ ) and WSR ( $\text{s}^{-1}$ ), for each field of view i.e. left nasal (LN), left temporal (LT), right nasal (RN) and right temporal (RT).

The correlation, expressed via the correlation coefficient ( $r$ ) and the best fit trend line, between increasing microvessel diameter and the haemodynamic measures Va, Q and WSR were consistent across the 4 fields of view, which are individually

illustrated in Fig.6a-d.



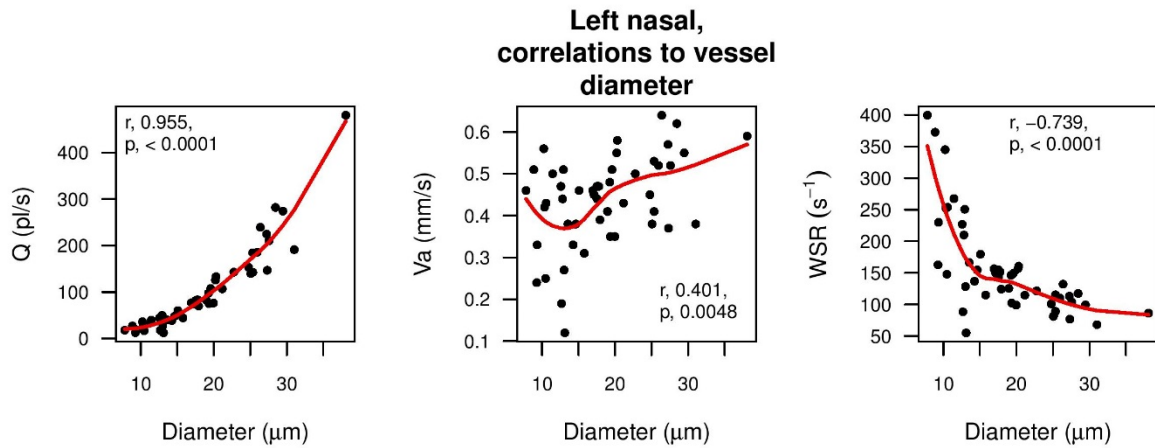


Fig.6. Correlation plots between microvessel diameter  $D$  ( $\mu\text{m}$ ) vs  $V_a$  (mm/s),  $Q$  (pl/s) and  $WSR$  ( $\text{s}^{-1}$ ) for each field of view ((a) RT, (b) RN, (c) LT, (d) LN).

A summary of the correlations between microvessel  $D$  and the quantified haemodynamic measures are illustrated in Fig.7. demonstrating the strong overall linear correlation with  $Q$  and  $WSR$  ( $r$  0.967,  $r$  -0.823 respectively). A modest correlation was seen for  $V_a$  ( $r$  0.404).

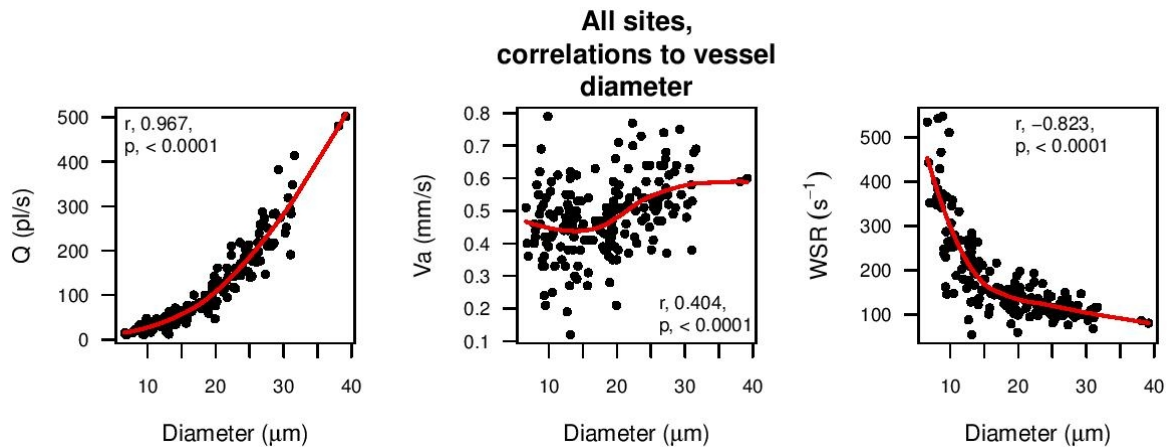


Fig.7. Correlation plots between microvessel diameter  $D$  ( $\mu\text{m}$ ) vs  $V_a$  (mm/s),  $Q$  (pl/s) and  $WSR$  ( $\text{s}^{-1}$ ) across all sites.

The correlations between increasing vessel diameter and  $V_a$ ,  $Q$ , and  $WSR$  are in keeping with that reported in previous work<sup>11,12</sup>, whereby similar fluid dynamics and microvascular relationships have been observed.

#### IV. Discussion

The conjunctival microcirculation represents a readily-accessible vascular network for non-invasive assessment. Physiological measures in the conjunctival microcirculation display the same trends and correlations as they do elsewhere in the circulation and, based on this rationale, may represent a key microcirculation that could be assessed in the evaluation of circulatory health and, if so, correlated with risk. Correlations between cardiovascular risk estimation and quantitative conjunctival haemodynamic measures, namely velocity and blood flow, were demonstrated in previous work<sup>21</sup>.

In recent years, there have been several reports regarding the clinical utility of conjunctival microcirculatory study. Conjunctival haemodynamic assessment has extended to patients with diabetes mellitus, in correlation with diabetic retinopathy status, with differences between Va, Q and WSR being observed for differing grades of retinopathy<sup>19</sup>. Quantitative assessment of the conjunctival haemodynamics was, also, evaluated in patients with ischaemic unilateral stroke and Va was found to be significantly lower in the ipsilateral eye to the stroke compared to the contralateral eye, demonstrating the physiological relationship shared by the internal carotid arterial system and the conjunctival microcirculation<sup>20</sup>.

We have described the application of smartphone technology, combined with a slit-lamp, in the quantitative assessment of conjunctival haemodynamics, namely D, Va, Q and WSR. With our approach, we have demonstrated the feasibility of obtaining haemodynamic results, similar to the correlations and trends described elsewhere by other groups using a digital charged coupled camera. We have done so, though, using a smartphone which served as an efficient, pragmatic and reliable means of

acquiring the conjunctival images for subsequent analysis. Our system performed as well as the more complex and time-consuming CCD devices and represents a potential major advancement within the scope of conjunctival microcirculation assessment. Our biomicroscope/smartphone apparatus and post-capture analysis is validated by comparison to results obtained previously. We obtained a mean diameter of 18.2µm (range 6.6-39.2µm) in 623 microvessels, selected manually according to the quality of STI, on post-processed images and these results are similar to, and within range, of that reported by other groups<sup>11</sup>. The strong positive/negative correlation between microvessel diameter (D) and blood flow (Q)/wall shear rate (WSR), reported in the present work, is reflective of the dependence of Q/WSR with increasing D, as represented in fluid dynamics formulae and observations reported in other studies<sup>11, 12,13</sup>. We did not find as strong a correlation for axial velocity (Va) and D ( $r = 0.404$ ), but it is important to note that the calculation of both D and Va, using our previously described methods, are entirely independent of each other and that similar relationships between D and Va have been reported previously<sup>12, 16</sup>. Statistical significance, though, was observed for group-4 vessels and their associated Va, compared to groups 1-3 ( $p < 0.0001$ ).

Combined smartphone and slit-lamp based quantitative assessment has been demonstrated in this present work and it is feasible that it could be of potential future application in the assessment of cardiovascular health. We studied a “low-cardiovascular risk” patient group, as evidenced by a mean QRISK 3 score of 6.6%. QRISK 3 is a well-validated 10-year cardiovascular risk assessment, with the largest sample size of contemporary cardiovascular estimation systems, implemented within major European guidelines<sup>30</sup>.

We acknowledge certain limitations of our study. We, similar to other feasibility studies<sup>13</sup>, have reported results for all visible microvessels without separating arterioles and venules. The feasibility of artery-vein classification, using our approach, in the conjunctiva requires further exploration, which we intend to pursue. In addition, cardiac-gated haemodynamic measures, primarily end-systolic and end-diastolic measures using conjunctival vessel pulse waveform characteristics, have been reported previously and could be of potential use in future clinical application with certain cardiovascular disease subsets<sup>35</sup>. A key aim of our future work is to implement and validate a fully automated smartphone-based approach to remove potential human error, promote consistency, and improve the efficiency of the examination. By quantifying the conjunctival haemodynamics our method potentially allows the inexpensive assessment of patients with established cardiovascular and systemic disease, with promise for improving the diagnosis, risk stratification and, potentially, evaluating disease status and treatment modification of cardiovascular disease(s). The addition of smartphone technology, with its application (APP) versatility, wealth of data management, and computerised machine learning algorithms, modernises the slit-lamp biomicroscope assessment of the conjunctival microcirculation.

## **V. Conclusion**

We have described, for the first time, the successful measurement of dynamic microcirculatory haemodynamic measures using smartphone technology combined with a slit-lamp biomicroscope. Our semi-automated method found a positive linear relationship between increasing microvessel diameter (D) and blood flow (Q). An inverse relationship was observed for wall shear rate WSR, a direct surrogate of

WSS. These findings corroborate prior ones, for the same haemodynamic measures, reported by groups using a CCD camera for image acquisition, and support the feasibility of our smartphone-derived approach. Image acquisition was performed without clinical complication in a group of patients with low cardiovascular risk. The ease and speed with which images were reliably acquired holds promise for the future clinical application of this smartphone-based conjunctival microcirculatory assessment model.

## **VI. Acknowledgements**

This project was funded by Northern Ireland Chest Heart and Stroke (NICHs), the Ulster University and the Heart Trust fund, Royal Victoria Hospital, Belfast, United Kingdom.

## **VII. Disclosure/Conflict of interests**

The authors, collectively, have no conflicts of interest or anything to disclose with respect to this original research manuscript.

## **VIII. Reference list**

1. Bhatnagar P, Wickramasinghe K, Williams J, et al. The epidemiology of cardiovascular disease in the UK 2014. *Heart*. 2015; 101:1182-1189
2. Stokes KY, and Granger DN. The microcirculation: a motor for the systemic inflammatory response and large vessel disease induced by hypercholesterolaemia? *J. Physiol*. 2005; 562:647–653

3. Krentz AJ, Clough G, Byrne CD. Vascular disease in the metabolic syndrome: Do we need to target the microcirculation to treat large vessel disease? *J Vasc Res.* 2009; 46:515–526
4. Liew G, Mitchell P, Rochtchina E, Wong TY, Hsu W, Lee ML, Wainwright A, Wang JJ. Fractal analysis of retinal microvasculature and coronary heart disease mortality. *Eur Heart J.* 2011; 32: 422–429
5. Cheung et al. Correlation of microvascular abnormalities and endothelial dysfunction in type-1 diabetes mellitus (T1DM): A realtime intravital microscopy study, *Clin. Hemorheol. Microcirc.* 2009; 42(4): 285–295
6. Wong TY, Klein R, Sharrett AR, Duncan BB, Couper DJ, Tielsch JM, Klein BE, Hubbard LD. Retinal arteriolar narrowing and risk of coronary heart disease in men and women. The Atherosclerosis Risk in Communities Study. *JAMA.* 2002; 287:1153–1159
7. Wanek J, Gaynes B, Lim JI, Molokie R, Shahidi M. Human bulbar conjunctival hemodynamics in haemoglobin SS and SC disease. *Am. J. Hematol.* 2013; 88(8): 661–664
8. Cheung et al. Microvascular abnormalities in sickle cell disease: A computer-assisted intravital microscopy study. *Blood.* 2002; 99(11):3999–4005
9. Houben AJHM, Martens RJH, Stehouwer CDA. Assessing microvascular function in humans from a chronic disease perspective. *JASN.* 2017; 28(12):3461-3472
10. Van Buskirk EM. The anatomy of the limbus. *Eye (Lond).* 1989; 3(2):101-8.

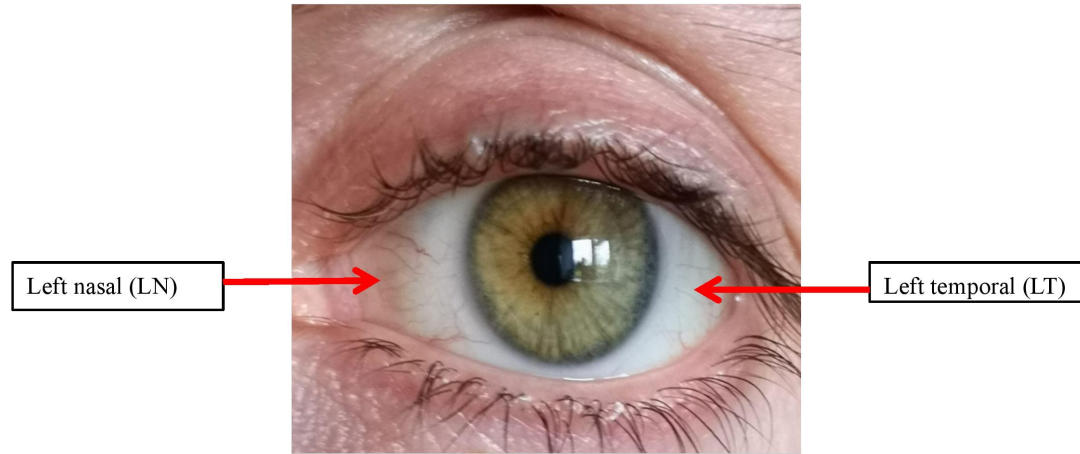


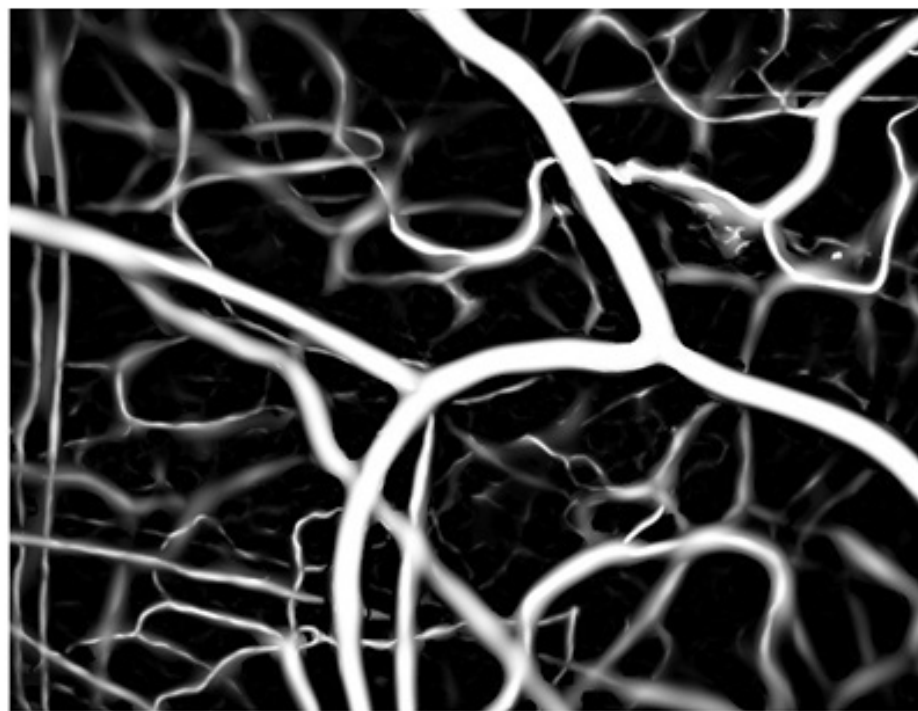
11. Khansari MM, Wanek J, Felder AE, Camardo N, Shahidi M. Automated assessment of hemodynamics in the conjunctival microvasculature network. *IEEE Transactions on Medical Imaging*. 2016; 35:605-611
12. Koutsiaris et al. Volume flow and wall shear stress quantification in the human conjunctival capillaries and post-capillary venules in vivo. *Biorheology*. 2007; 44(5): 375–386
13. Shahidi M, Wanek J, Gaynes B, Wu T. Quantitative assessment of conjunctival microvascular circulation of the human eye. *Microvasc Res*. 2010; 79(2):109-13
14. Koutsiaris AG, Tachmitzi SV, Papavasileiou P, Batis N, Kotoula MG, Giannoukas AD, Tsironi E. Blood velocity pulse quantification in the human conjunctival pre-capillary arterioles. *Microvasc Res*. 2010; 80(2):202-8
15. Kord Valeshabad et al. Conjunctival microvascular haemodynamics in sickle cell retinopathy. *Acta Ophthalmol* 2015; 93(4):275-80
16. Jiang et al. Functional slit lamp biomicroscopy for imaging bulbar conjunctival microvasculature in contact lens wearers. *Microvascular Res*. 2014; 92:62-71
17. Wang L, Yuan J, Jiang H, Yan W, Cintron-Colon H, Perez V, Cabrerra DeBuc D, Feuer W, Wang J. Vessel sampling and blood flow velocity distribution with vessel diameter for characterizing the human bulbar conjunctival microvasculature. *Eye Contact Lens*. 2016; 42(2): 135–140.

18. To et al. Real-time studies of hypertension using non-mydriatic fundus photography and computer-assisted intravital microscopy. *Clin. Hemorheol. Microcirc.* 2013; 53(3): 267–279
19. Khansari et al. Assessment of Conjunctival Microvascular Hemodynamics in Stages of Diabetic Microvasculopathy. *Sci Rep.* 2017; 7:45916
20. Kord Valeshabad A, Wanek J, Mukarram F, Zelkha R, Testai FD, Shahidi M. Feasibility of Assessment of Conjunctival Microvascular Hemodynamics in Unilateral Ischemic Stroke. *Microvasc Res.* 2015; 100:4–8
21. Karanam VC, Tamariz L, Batawi H, Wang J, Galor A. Functional slit lamp biomicroscopy metrics correlate with cardiovascular risk. *The Ocular Surface.* 2019; 17:64-69
22. Proesman T, Nuyens D, Vandervoort P, Van Herendael H, Rivero-Ayerza M. First results from a digital mass screening for atrial fibrillation using a smartphone application. *Circulation.* 2018; 138(1):A15960
23. Rajalakshmi R et al. Automated diabetic retinopathy detection in smartphone-based fundus photography using artificial intelligence. *Eye.* 2018; 32:1138-1144
24. Russo A, Morescalchi F, Costagliola C, Delcassi L, Semeraro F. A novel device to exploit the smartphone camera for fundus photography. *J Ophthalmol.* 2015; 823139
25. Muiesan ML, Salvetti M, Paini A, Riviera M, Pintossi C, Bertacchini F, Colonetti E, Agabiti-Rosei C, Poli M, Semeraro F, Agabiti-Rosei E,

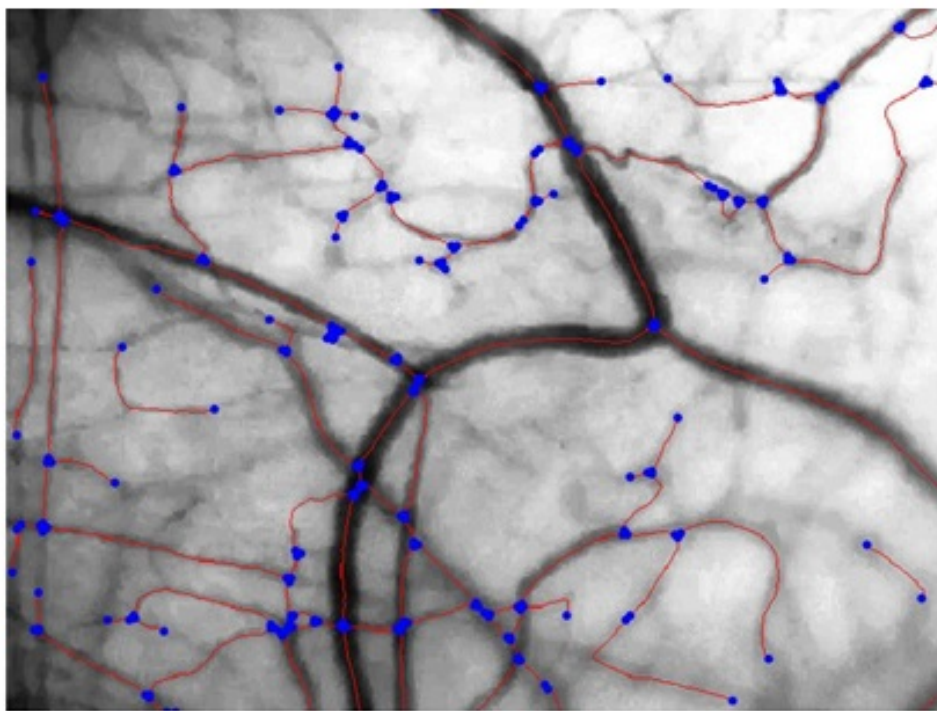
- Russo A. Ocular fundus photography with a smartphone device in acute hypertension. *J Hypertens*. 2017; 35:1660–1665
26. Collings S, Thompson O, Hirst E, Goossens L, George A, Weinkove R. Non-Invasive Detection of Anaemia Using Digital Photographs of the Conjunctiva. *PLoS ONE*. 2016; 11(4): e0153286
27. Tamir, C. S. Jahan, M. S. Saif, S. U. Zaman, M. M. Islam, A. I. Khan and C. Shahnaz. Detection of anemia from image of the anterior conjunctiva of the eye by image processing and thresholding, *In Humanitarian Technology Conference (R10-HTC), 2017 IEEE Region 10*, pp. 697-701, 2017.
28. Otero C, Garcia-Porta N, Tabernero J, Pardhan S. Comparison of different smartphone cameras to evaluate conjunctival hyperaemia in normal subjects. *Scientific Reports*. 2019; 9(1):1339
29. Gottemukkula, V., Saripalle, S., Tankasala, S. P., & Derakhshani, R. Method for using visible ocular vasculature for mobile biometrics. *IET Biometrics*. 2016; 5(1):3-12.
30. Piepoli et al. 2016 European Guidelines on cardiovascular disease prevention in clinical practice. ESC Guidelines. *European Heart Journal*. 2016; 37(29):2315-2381
31. Forsberg D. Robust image registration for improved clinical efficiency: Using local structure analysis and model-based processing PhD thesis, Linköping University, Medical Informatics, The Institute of Technology, Center for Medical Image Science and Visualisation (CMIV). 2013

32. Jerman AFT, Pernus F, Likar Z, Spiclin Z. Enhancement of vascular structures in 3D and 2D angiographic images. *IEEE Transactions on Medical Imaging*. 2016; 35(9):2108-2118
33. Duval-Destin M, Murenzi R. "Spatio-Temporal Wavelet: Application to the Analysis of Moving Patterns, in Progress in Wavelets Analysis and Applications. *FrontiReres, Gif-sur-Yvette*. 1993;399-408
34. Jacques L, Coron A, Vandergheynst P, Rivoldini A. The YAWTb toolbox: Yet another wavelet toolbox. 2001.  
<https://sites.uclouvain.be/ispgroup/yawtb/doc/YAWTBReferenceManual.pdf>
35. Koutsiaris AG, Tachmitzi S, Batis N. Wall shear stress quantification in the human conjunctival pre-capillary arterioles in vivo. *Microvascular Research*. 2013; 85;34–39
36. Pries AR, Secomb TW, Gaehtgens P. Design Principles of Vascular Beds. *Circ Res*. 1995b; 77:1017–1023
37. Ricci S, Swillens A, Ramalli A, Segers P, Tortoli P. Wall Shear Rate Measurement: Validation of a New Method Through Multiphysics Simulations. *IEEE Trans Ultrason Ferroelectr Freq Control*. 2017; 64(1):66-77

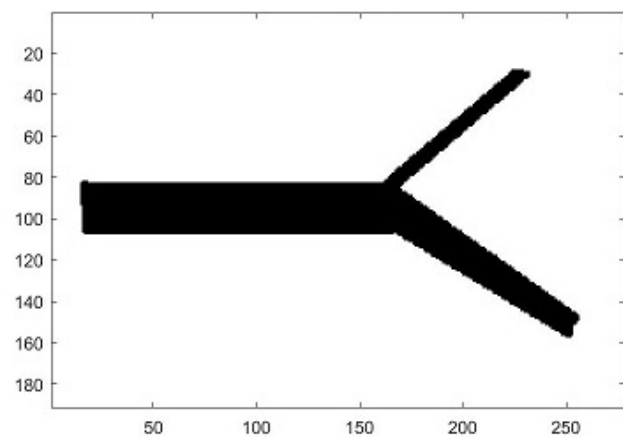




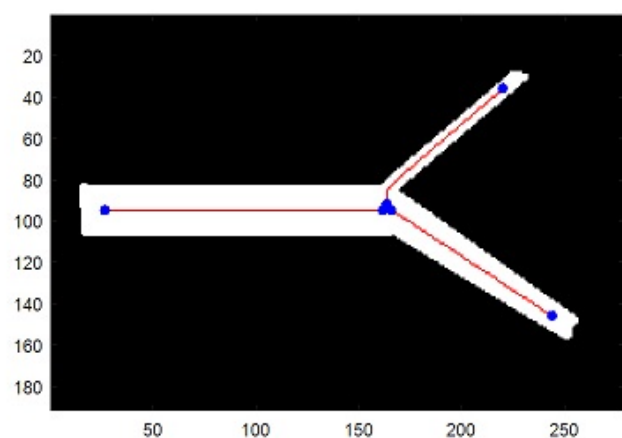
(a)



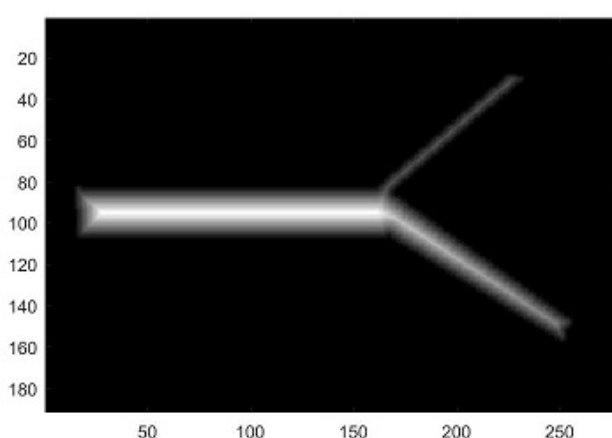
(b)



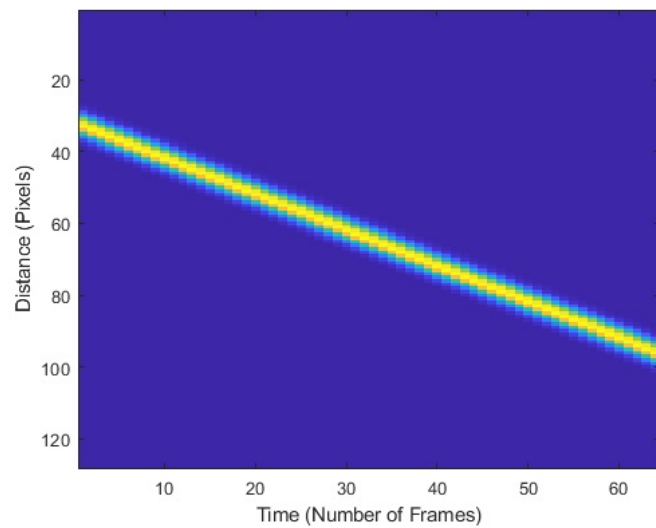
(a)



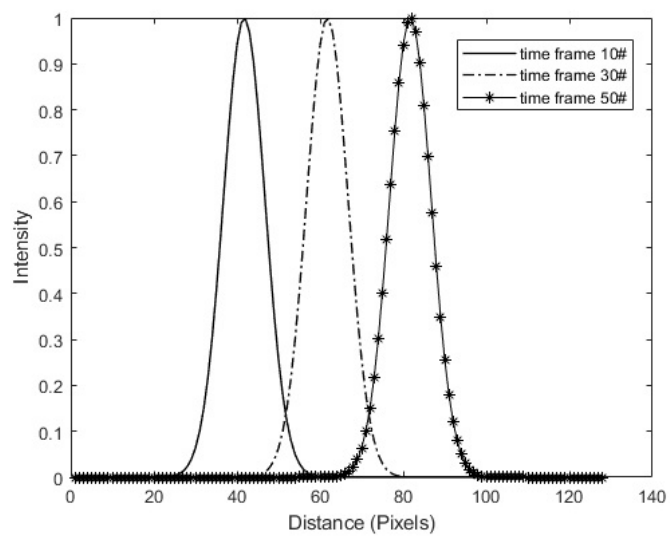
(b)



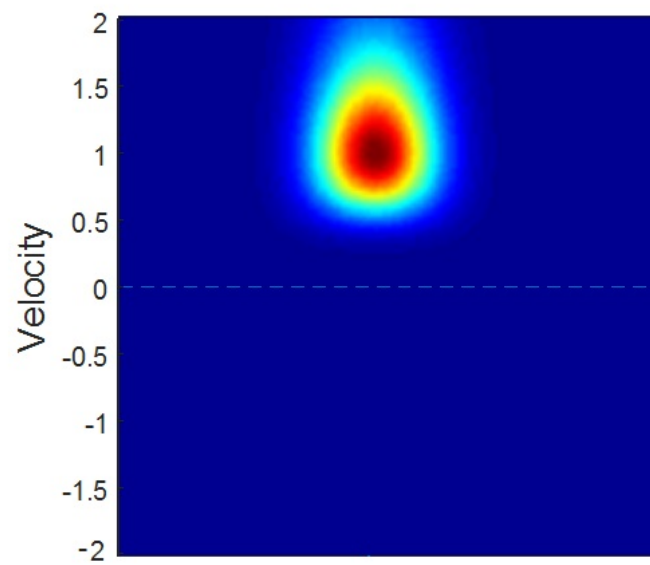
(c)



(a)



(b)

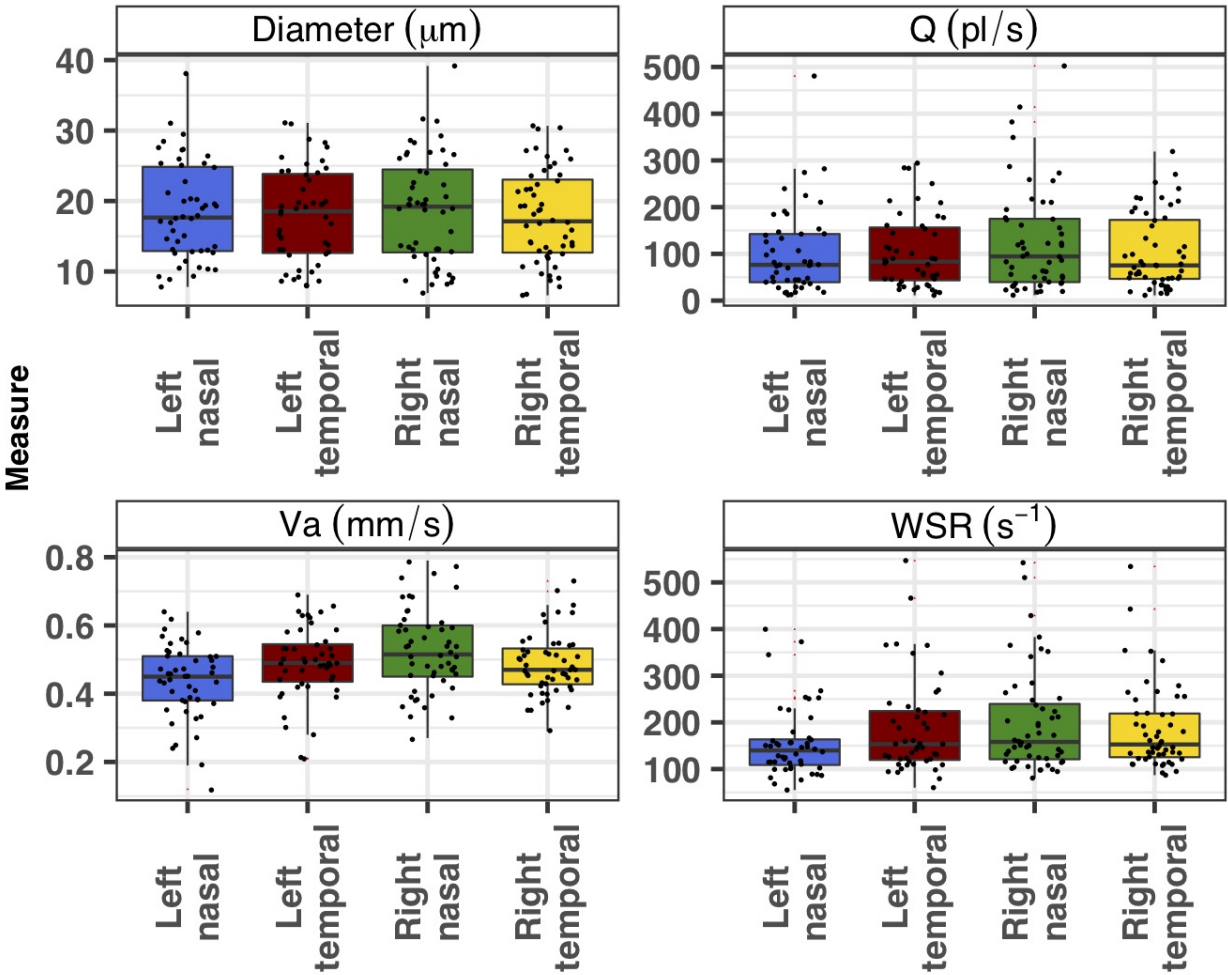


(c)

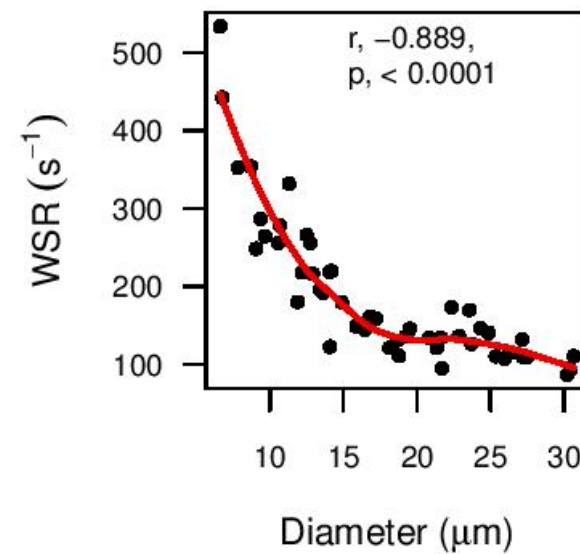
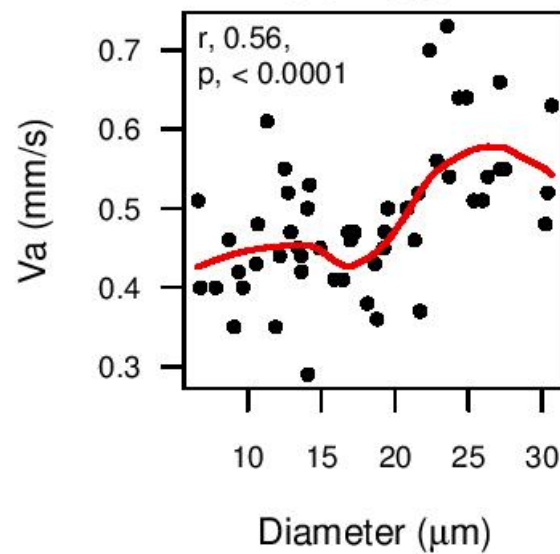
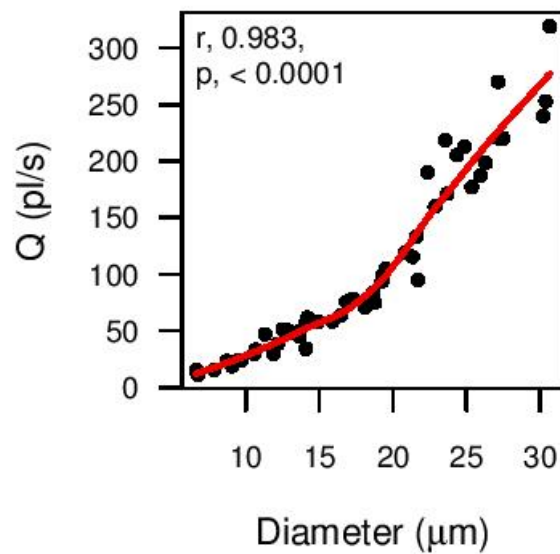


Diameter, Q, Va, and WSR across site

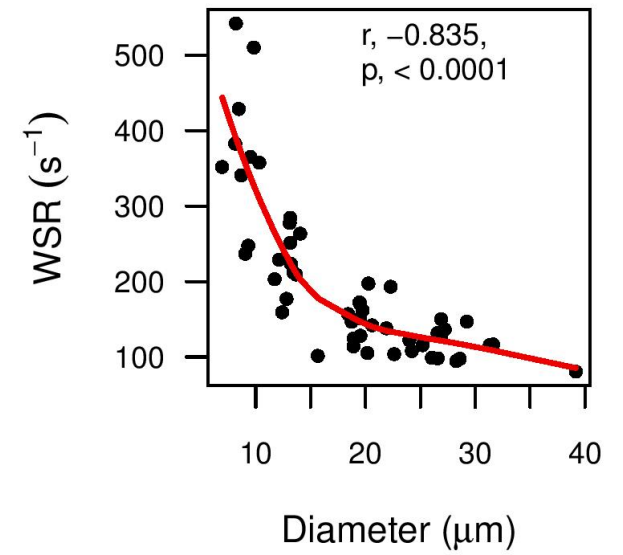
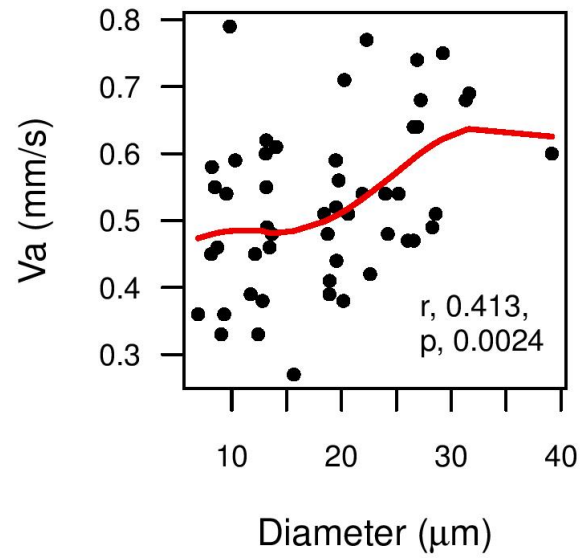
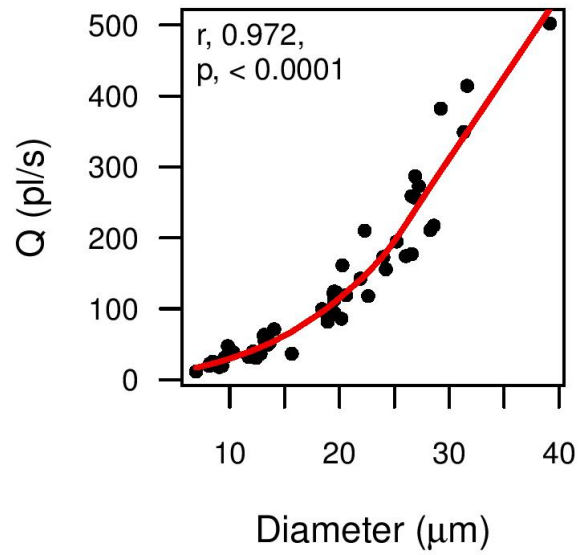
Site     Left nasal     Left temporal     Right nasal     Right temporal



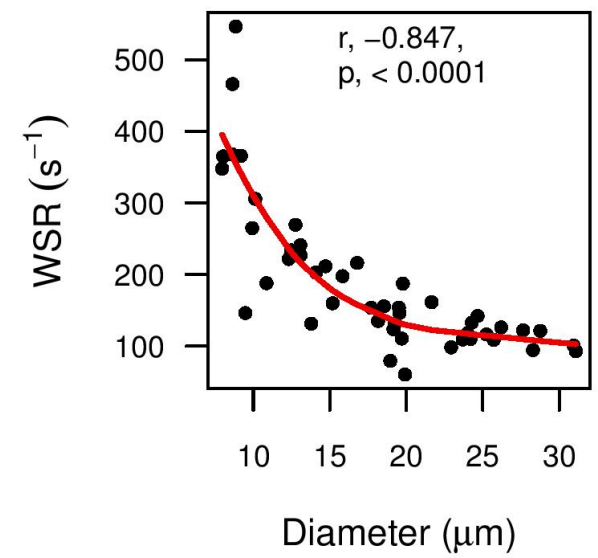
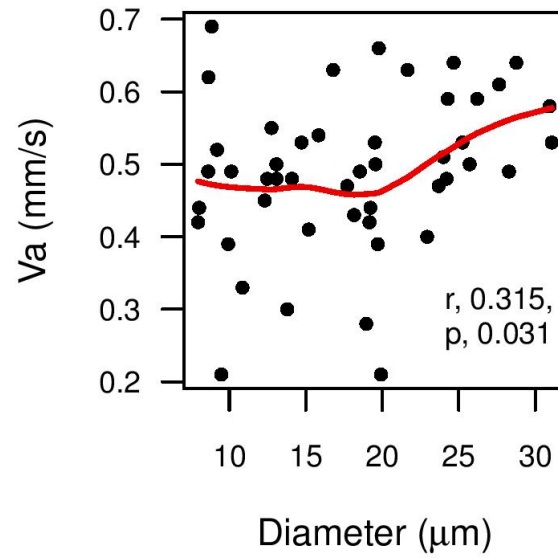
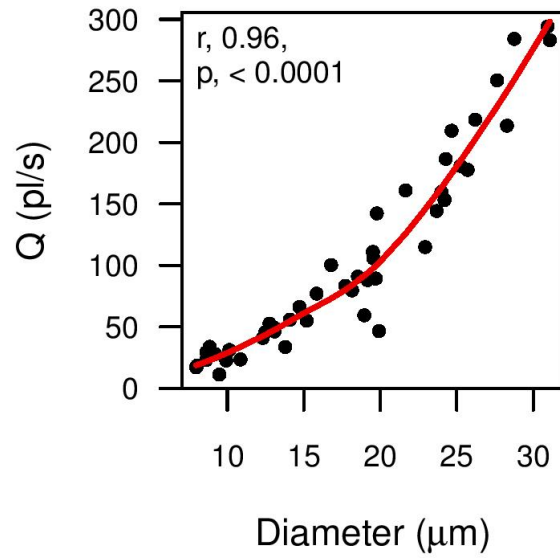
**Right temporal,  
correlations to vessel  
diameter**



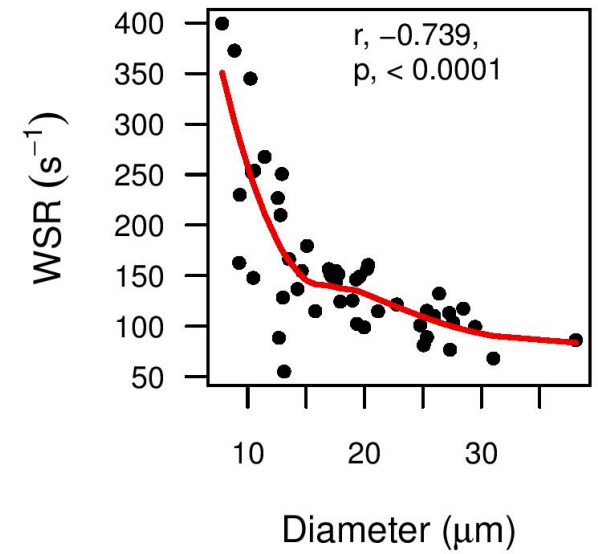
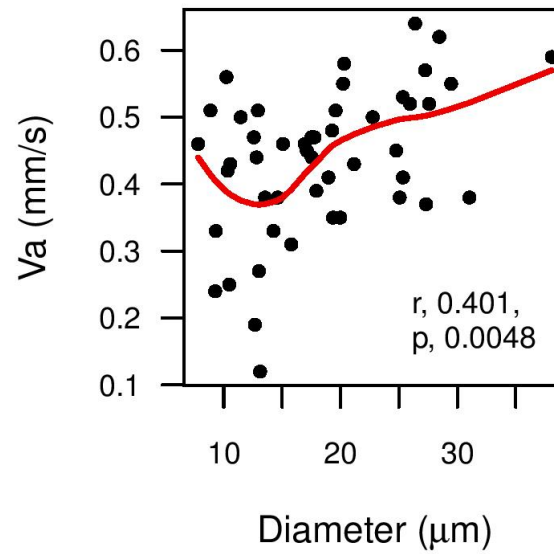
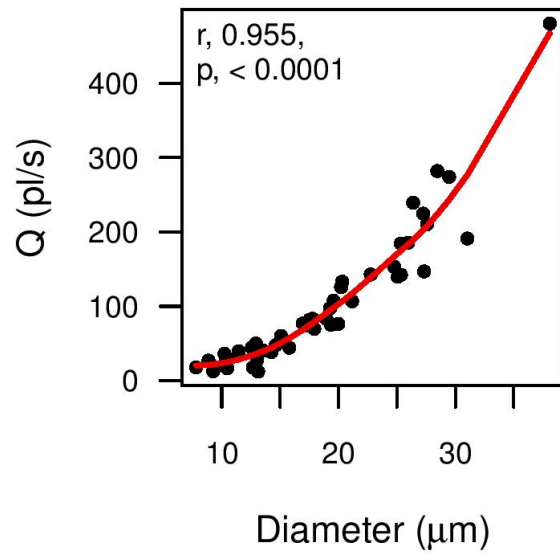
**Right nasal,  
correlations to vessel  
diameter**



**Left temporal,  
correlations to vessel  
diameter**



# Left nasal, correlations to vessel diameter



**All sites,  
correlations to vessel  
diameter**

